ЖЭТФ/JETP, 2026, том 169, вып. 2, стр. 212–224

MAGNETIC RESONANCE IN NANOGRANULAR COMPOSITES: OBSERVATION AND PROPERTIES OF «DOUBLE QUANTUM» EXCITATIONS IN FERROMAGNETIC PARTICLES

A. B. Drovosekov [a*], ***M. Yu. Dmitrieva*** [a,b], ***A. V. Sitnikov*** [c,d], ***S. N. Nikolaev*** [d], ***V. V. Rylkov*** [d,e,f]

[a] *P. L. Kapitza Institute for Physical Problems, Russian Academy of Sciences 119334, Moscow, Russia*

[b] *National Research University Higher School of Economics 101000, Moscow, Russia*

[c] *Voronezh State Technical University 394026, Voronezh, Russia*

[d] *National Research Center Kurchatov Institute 123182, Moscow, Russia*

[e] *Institute of Theoretical and Applied Electrodynamics, Russian Academy of Sciences 125412, Moscow, Russia*

[f] *Kotelnikov Institute of Radio Engineering and Electronics, Fryazino Branch, Russian Academy of Sciences 141190, Fryazino, Moscow region, Russia*

Received December 8, 2025,
revised version December 8, 2025
Accepted for publication December 9, 2025

Films of metal-insulator nanogranular composites $(CoFeB)_x(Al_2O_3)_{100-x}$ and $(CoFeB)_x(SiO_2)_{100-x}$ with different content of metal ferromagnetic phase CoFeB ($x \approx 20{-}60$ at. %) are investigated by electron spin resonance. The experiments are carried out in a wide range of frequencies ($f = 7{-}80$ GHz) and temperatures ($T = 4.2{-}360$ K) at different orientations of the magnetic field (up to 24 kOe) with respect to the film plane. Besides the conventional ferromagnetic resonance signal, the experimental spectra contain a weak additional absorption peak which is characterized by a double effective g-factor $g_{eff} \approx 4$ and demonstrates a number of other unusual properties. The appearance of such a peak in the resonance spectra can be explained in the framework of the quantum mechanical «giant spin» model by the excitation of «forbidden» («double quantum») transitions in magnetic nanogranules with a change of the spin projection $\Delta m = \pm 2$. Here we study the applicability of this model to explain anomalous behavior of the $g_{eff} \approx 4$ resonance peak, as well as discuss a classical interpretation of the observed phenomena. In particular, the influence of dipolar fields in the films on the frequency-field dependencies for the «double quantum» absorption peak is of interest.

Keywords: magnetic nanoparticles, superparamagnetism, electron spin resonance

DOI: 10.7868/S3034641X26020088

1. INTRODUCTION

Magnetic nanoparticles and nanogranular structures exhibit unusual physical properties which are not typical of massive magnetic crystals, attracting the attention of researchers from both fundamental and applied points of view [1–3]. An interesting concept associated with magnetic nanoparticles is the quantum-classical duality of their nature. Within the framework of this concept, a magnetic nanoparticle is considered as an object occupying an intermediate position be-

* E-mail: drovosekov@kapitza.ras.ru

tween an isolated paramagnetic (PM) ion (quantum object) and a macroscopic ferromagnet (classical object). The well-known phenomenon of superparamagnetism in nanoparticle ensembles can be interpreted as one of the manifestations of such duality. More nontrivial effects of quantum mechanical nature are manifested in magnetic resonance studies of nanoparticles [4–12].

In the works [13–16] we studied magnetic resonance in films of metal-insulator nanogranular composites M_xD_{100-x} with different compositions and percentage ratio x of metal («M») and dielectric («D») phases. The studied structures represent an array of ferromagnetic (FM) metallic nanogranules randomly distributed in a solid-state insulating medium (matrix). It was found that in addition to the usual ferromagnetic resonance (FMR) signal, the experimental spectra contained an additional «anomalous» absorption peak demonstrating a number of unusual properties: double effective g-factor $g_{eff} \approx 4$, non-standard conditions for its excitation by longitudinal microwave (MW) magnetic field, and nonmonotonic dependencies of the peak intensity on temperature.

Initially [13–15], the observed unusual peak was ascribed to electron paramagnetic resonance (EPR) of isolated ions Fe^{3+} dispersed in the dielectric medium between FM granules. Indeed, the presence of EPR peak with $g_{eff} \approx 4.3$ is quite common for systems containing Fe^{3+} ions [2,5,17–20]. However, in our case, the anomalous behavior of the observed peak could not be explained satisfactorily within this approach.

In the work [16], it was shown that many of the observed features of the spectra can be well explained if we consider FM nanogranules as quantum objects (PM centers) with a «giant» ($S \sim 10^2$–10^4) spin [4–12]. Within this approach, the appearance of a resonance peak with effective g-factor $g_{eff} \approx 4$ is associated with the excitation of «double quantum» transitions in the granules with a change in the spin projection $\Delta m = \pm 2$. More detailed discussions of this model and its experimental consequences are given below in Section 3.

This work is devoted to further investigation of the applicability of the concept of «multiple quantum» transitions for describing the magnetic resonance features of nanogranular composites. In particular, we develop classical interpretation of the quantum mechanical «giant spin» model. On this basis, we demonstrate a principally different influence of dipolar fields in nanocomposite films on the resonance frequency shift for the conventional FMR line and the «double quantum» peak.

2. SAMPLES AND EXPERIMENTAL TECHNIQUES

Nanocomposite films of about 1 μm thickness with the nominal composition $(CoFeB)_x(Al_2O_3)_{100-x}$ and $(CoFeB)_x(SiO_2)_{100-x}$ were synthesized on glass-ceramic substrates by ion-beam sputtering of composite targets [21, 22]. The content of the metallic ferromagnetic phase $Co_{40}Fe_{40}B_{20}$ (CoFeB) for different samples varied within $x \approx 20$–60 at. % according to the data of energy dispersive X-ray microanalysis.

Transmission electron microscopy of synthesized structures indicates that the obtained composites consist of FM nanogranules CoFeB randomly distributed inside the amorphous insulating oxide matrix [22, 23]. The granules have approximately spherical shape and their average size (2–8 nm) increases smoothly with a growth of the FM phase content x in the nanocomposite. The number of magnetic atoms in the granules can be estimated to change from $\sim 10^2$ to $\sim 10^4$ in the investigated range of concentrations x.

The electron transport and static magnetic properties of the structures were investigated in sufficient detail [22–25]. The percolation threshold of the composites under study lies in the vicinity of metal phase content $x \sim 50$ at. %. According to static magnetization data, the transition of the samples from superparamagnetic to ferromagnetic behavior occurs approximately in the same concentration range.

In this work, the nanocomposite samples are studied by electron spin resonance in a wide range of frequencies $f = 7$–80 GHz and temperatures $T = 4.2$–360 K. The experimental spectra are recorded sweeping the magnetic field (up to 24 kOe) at different directions with respect to the film plane. In the frequency range 7–38 GHz, a transmission-type spectrometer based on rectangular and tunable cylindrical cavity resonators is used [13]. In the range 25–80 GHz, a reflection from a shorted rectangular waveguide with the studied sample inside is measured. When the static magnetic field $\mathbf{H}$ is applied in the film plane, there is a possibility to apply the high-frequency field $\mathbf{h}$ either perpendicular ($\mathbf{h} \perp \mathbf{H}$) or parallel ($\mathbf{h} \parallel \mathbf{H}$) to the static field («transverse» and «longitudinal» resonance excitation geometries).

3. THEORETICAL REMARKS

3.1. Quantum mechanical «giant spin» model

In the works [4–12], the appearance of a peak with a double effective g-factor $g_{eff} \approx 4$ in magnetic reso-

nance spectra of superparamagnetic nanoparticles was explained within the framework of the quantum mechanical «giant spin» model. In this model, the FM nanogranule is treated as a PM center with a very large spin $S \sim 10^2{-}10^4$. In an external field H, Zeeman splitting of the energy levels of this spin occurs, according to its projection $m = -S... + S$ onto the field direction (z-axis). An alternating MW magnetic field h applied perpendicular to the static field at the resonance frequency $\omega_0 = \gamma H$, where γ is the gyromagnetic ratio, leads to forced transitions between neighboring energy levels of the granules ($\Delta m = \pm 1$). The probability amplitude of such «single quantum» transitions A_m^{m+1} is determined by non-diagonal elements of the spin matrices $\hat{S}_{\pm}$:

$$A_m^{m+1} = \sqrt{S(S+1) - m(m+1)}.$$

In the «giant spin» approximation $S \gg 1$, this value takes a simplified normalized form

$$\frac{A_m^{m+1}}{S} \approx A_1 = \sqrt{1 - m_z^2}, \tag{1}$$

where $m_z = -m/S$ is the projection of the unit magnetization vector onto the z-axis. Thus, in the classical limit, the probability amplitude of «single quantum» transitions A_1 is proportional to the amplitude of the magnetization vector precession around the field direction.

If only Zeeman splitting of the spin multiplet in a magnetic field is considered, the «multiple quantum» transitions with $\Delta m = \pm 2, \pm 3, \ldots$ are forbidden by the angular momentum conservation law. However, such transitions become possible in the presence of additional anisotropic interactions in the system, for example, in the presence of magnetic anisotropy of granules or intergranular dipole-dipole interactions [26, 27]. In this case, the angular momentum can exchange between the spin subsystem and the crystal, which allows the transitions with $\Delta m = \pm 2, \pm 3, \ldots$ inside the spin multiplet. Moreover, such «multiple quantum» transitions can be excited by MW field oriented both perpendicular and parallel to the static field.

Let us consider the simplest case of a weak uniaxial anisotropy in the nanogranules with effective field $H_A \ll H$. Such anisotropy can arise in the granules due to their non-spherical shape, crystalline structure, or surface effects [4]. In the framework of perturbation theory, the probability amplitude of «double quantum» transitions between the levels $m \leftrightarrow m + 2$ is proportional to [28, 29]

$$A_m^{m+2} = \frac{H_A}{H} \frac{A_m^{m+1} A_{m+1}^{m+2}}{4S} p(\theta),$$

where $p(\theta)$ is a function of angle θ between the anisotropy axis and the external field, depending on the resonance excitation geometry:

$$p(\theta) = \begin{cases} \sin 2\theta & \text{for } \mathbf{h} \perp \mathbf{H}, \\ \sin^2 \theta & \text{for } \mathbf{h} \parallel \mathbf{H}. \end{cases} \tag{2}$$

In the «giant spin» approximation $S \gg 1$, the probability amplitude of the «double quantum» transitions A_2 is proportional to the square of the classical magnetization vector precession amplitude A_1:

$$\frac{A_m^{m+2}}{S} \approx A_2 = \frac{1}{4} \frac{H_A}{H} A_1^2 p(\theta). \tag{3}$$

Thus, the presence of anisotropy allows for «double quantum» excitations in magnetic particles.

3.2. Classical interpretation

The discussed quantum mechanical approach has a simple classical analogy. The magnetic moment of a classical particle placed in an external field H performs a circular precession with a frequency $\omega_0 = \gamma H$. At this frequency, a conventional resonance occurs when a transverse MW field is applied. The presence of magnetic anisotropy in the particle leads to a distortion of the circular orbit of magnetization precession and the appearance of multiple harmonics of the precessional motion. Under these conditions, resonance absorption of MW power is also possible at the corresponding multiple frequencies.

According to the general properties of quasi-classical approximation, the quantum mechanical transition amplitudes in classical limit transform to Fourier components of classical motion at corresponding frequencies [30]. Let us demonstrate it directly solving the classical Landau – Lifshitz equations.

Similar to the quantum mechanical problem described above, we consider a classical magnetic particle with a weak uniaxial anisotropy. We introduce a coordinate system such that the z-axis is directed along the external field, and the anisotropy axis is oriented in the xz-plane at an angle θ to the field. The energy expression is

$$E = -\mu \left[H m_z + (H_A/2)(m_x \sin\theta + m_z \cos\theta)^2 \right], \tag{4}$$

where μ is the particle magnetic moment. The Landau – Lifshitz equations for the unit magnetization vector $\mathbf{m}$ will have the form

$$\begin{aligned}\dot{m}_x &= -m_y - a\left[2m_z m_y \cos^2\theta + m_x m_y \sin 2\theta\right],\\ \dot{m}_y &= m_x + a\left[2m_z m_x \cos 2\theta + (m_x^2 - m_z^2)\sin 2\theta\right], \quad (5)\\ \dot{m}_z &= a\left[m_z m_y \sin 2\theta + 2m_x m_y \sin^2\theta\right].\end{aligned}$$

Here we introduced a parameter $a = H_A/2H$ and dimensionless time derivatives

$$\dot{m}_\alpha = \omega_0^{-1} dm_\alpha/dt,$$

where $\alpha = x, y, z$.

We solve the resulting non-linear system as an expansion in powers of the small parameter $a \ll 1$. The mathematical aspects of this approach are described in [31, 32]. In «zero» approximation ($a = 0$), the solution of the system is obvious:

$$m_x = A_1 \cos\psi, \quad m_y = A_1 \sin\psi, \quad m_z = \text{const},$$

where $\psi = \omega_0 t + \varphi$. The precession phase φ is determined by the initial orientation of the magnetization vector, and the amplitude A_1 is connected with m_z by expression $A_1 = (1 - m_z^2)^{1/2}$ which, obviously, coincides with the quasi-classical Eq. (1).

In the first order in a, the solution of the system (5) takes the form of Fourier expansion up to the second harmonic (for more details, see Appendix):

$$\begin{aligned}m_{x,z} &= \bar{m}_{x,z} + A_{1x,z}\cos\psi + A_{2x,z}\cos 2\psi,\\ m_y &= A_{1y}\sin\psi + A_{2y}\sin 2\psi.\end{aligned} \quad (6)$$

Here $\psi = \omega_1 t + \varphi$, where φ is determined by initial conditions, and the main frequency ω_1 is corrected as compared to ω_0:

$$\omega_1 = \omega_0\left[1 + \frac{1}{2}\frac{H_A}{H}\bar{m}_z(3\cos^2\theta - 1)\right] \quad (7)$$

(see also [4]). In the xy-plane, the precession orbit takes elliptical form, while an oscillating z-component of magnetization arises at the main frequency ω_1:

$$\begin{aligned}A_{1x,y} &= A_1\left(1 \pm \frac{1}{4}\frac{H_A}{H}\bar{m}_z \sin^2\theta\right),\\ A_{1z} &= -\frac{1}{2}\frac{H_A}{H}A_1\bar{m}_z \sin 2\theta.\end{aligned} \quad (8)$$

At the same time, a non-zero harmonic at double frequency $\omega_2 = 2\omega_1$ appears. Its amplitude components by coordinates:

$$\begin{aligned}A_{2x,y} &= \frac{1}{4}\frac{H_A}{H}A_1^2 \sin 2\theta,\\ A_{2z} &= -\frac{1}{4}\frac{H_A}{H}A_1^2 \sin^2\theta.\end{aligned} \quad (9)$$

The amplitude A_1 in Eqs. (8), (9) is defined by Eq. (1), where m_z must be replaced by its time-averaged value $\bar{m}_z$. As we can see, the second harmonics $A_{2\alpha}$ of the classical magnetization precession exactly reproduce Eqs. (2), (3) for the probability amplitudes of double quantum transitions in the «giant spin» model.

3.3. Linear response to microwave field

Now let us consider a statistical ensemble of magnetic particles described by Eqs. (5) placed in MW magnetic field $\mathbf{h}$. The average absorption power Q per unit particle is given by

$$Q = -\mu\left\langle \mathbf{m}\, d\mathbf{h}/dt\right\rangle,$$

where brackets $\langle ... \rangle$ denote the thermal averaging. In the usual way [33, 34], this power can be associated with the imaginary part of the generalized susceptibility $\chi''(\omega)$ which describes the linear relation between Q and the MW field energy $\sim h^2$:

$$Q = \frac{1}{2}\omega h^2 \chi''(\omega).$$

According to the fluctuation-dissipation theorem, $\chi''(\omega)$ is related to the Fourier transform of the correlation function $\langle m_\alpha(0)\, m_\alpha(t)\rangle$ [33, 34]:

$$\chi''(\omega) = \frac{\omega}{2k_B T}\,\mu^2 \int\limits_{-\infty}^{\infty} \langle m_\alpha(0)\, m_\alpha(t)\rangle\, e^{i\omega t} dt,$$

where $m_\alpha(t)$ is a variable component of unit magnetization vector parallel to $\mathbf{h}$ and k_B is Boltzmann constant. Substituting $m_\alpha(t)$ in the form of Fourier series (see Eqs. (6)) and taking into account that the precession phase φ is random, we get

$$\chi''(\omega) = \frac{\pi}{4}\frac{\omega}{k_B T}\,\mu^2 \sum_q \left\langle A_{q\alpha}^2 \delta(\omega - \omega_q)\right\rangle.$$

Thus, the susceptibility $\chi''(\omega)$ represents a set of absorption peaks at multiple resonance frequencies $\omega_q \approx q\omega_1$. In the limit of identical precession frequencies ω_1 for all particles and infinite relaxation time τ, the peaks have the shape of delta functions $\delta(\omega - \omega_q)$. In the real situation, the peaks are broadened due to the spread of ω_1 (see Eq. (7)) and the presence of thermal fluctuations (finite τ). Nevertheless, in the limit of narrow peaks ($H_A \ll H$, $\omega^{-1} \ll \tau$), their integral intensities are defined by thermal averaging of squared harmonics $\left\langle A_{q\alpha}^2\right\rangle$.

Further we concentrate our interest on the intensity of a weak second harmonic peak ($A_2 \sim A_2/A_1 \sim a$).

In this situation, with a sufficient accuracy, the thermal distribution function ρ_0 can be considered in «zero» approximation, taking into account only Zeeman energy contribution $E = -\mu H m_z$. Then, the peak intensities are estimated to be proportional to

$$I_q = \frac{\varkappa}{2} \int_{-1}^{1} A_{q\alpha}^2 \, \rho_0 \, dm_z, \qquad (10)$$

where [35]

$$\rho_0 = \frac{\varkappa}{2 \operatorname{sh} \varkappa} e^{\varkappa m_z}, \quad \varkappa = \frac{\mu H}{k_B T}.$$

In the case of the main resonance peak ($q = 1$) excited by transverse MW field, Eq. (10) in «zero» approximation yields the Langevin function $I_1 = L(\varkappa) = \coth \varkappa - \varkappa^{-1}$. For the intensity of «double quantum» excitations ($q = 2$), taking into account Eqs. (9):

$$I_2 = \frac{1}{4} \left(\frac{H_A}{H} \right)^2 \frac{\varkappa - 3L(\varkappa)}{\varkappa^2} p^2(\theta).$$

This expression reproduces the result obtained within the «giant spin» model [6, 7]. In the case of arbitrary orientations of anisotropy axes in magnetic particles, averaging the function $p^2(\theta)$ over the total solid angle $\Omega = 4\pi$ yields

$$\langle p^2(\theta) \rangle_\Omega = \frac{1}{4\pi} \int p^2(\theta) \, d\Omega = \frac{8}{15}$$

regardless of the orientation of the MW field with respect to the static one. Thus, the intensity of the «double quantum» absorption line does not depend on the resonance excitation geometry and is determined by

$$I_2 = \frac{2}{15} \left(\frac{H_A}{H} \right)^2 \frac{\varkappa - 3L(\varkappa)}{\varkappa^2}. \qquad (11)$$

As an example, Fig. 1 demonstrates experimental resonance spectra for one of the studied films measured at different orientations of the MW field **h** relative to **H**. We see that the intensity of the main peak («FMR») is proportional to the square of the transversal component of **h**. The second peak is located at about half-field with respect to the main peak and its intensity does not depend on the **h** orientation. This behavior is in accordance with the theoretical prediction for the «double quantum» resonance line.

One more interesting feature of the function (11) is its non-monotonic temperature dependence. At low temperatures ($\varkappa \gg 1$), Eq. (11) gives linear dependence $I_2 \propto T$. At high temperatures ($\varkappa \ll 1$), $I_2(T)$ follows the Curie law $I_2 \propto T^{-1}$. The maximal value I_2 is achieved at $T_{max} \approx 0.29 \, \mu H / k_B$ which is dependent on the particle magnetic moment μ (the resonance field H is defined by experimental frequency).

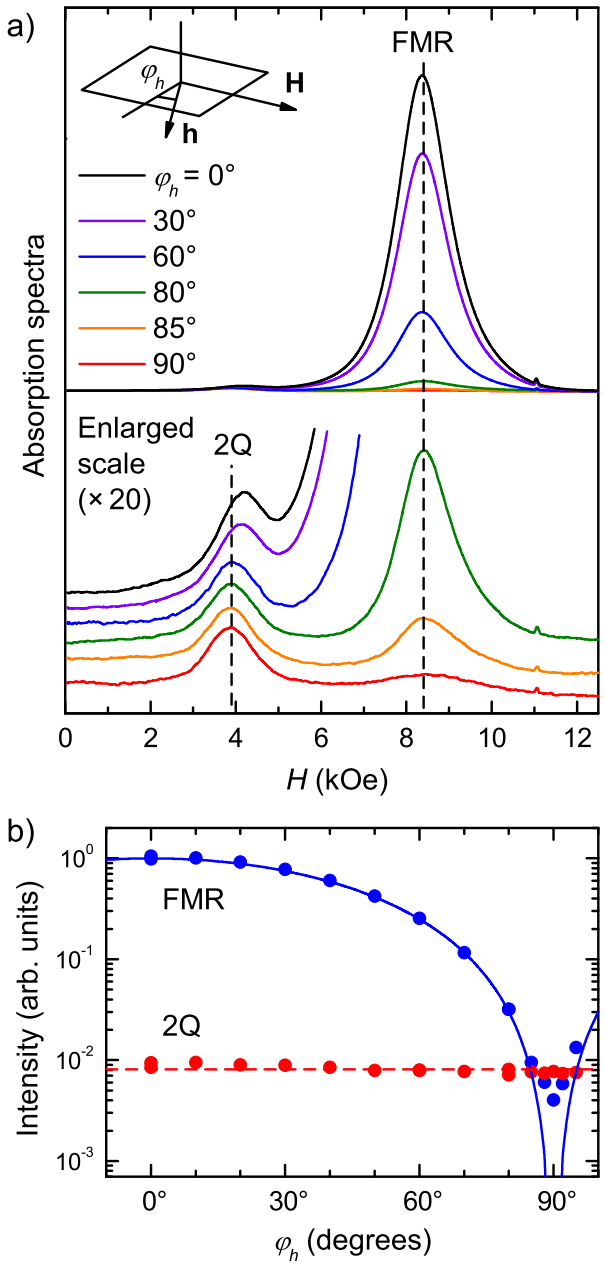

Fig. 1. *a* — Room temperature absorption spectra for the film $(CoFeB)_{40}(Al_2O_3)_{60}$ at a frequency $f \approx 31.0$ GHz when changing the resonance excitation geometry from transverse (φ_h=0) to longitudinal (φ_h=90°). *b* — Integral intensities of the FMR line and the «double quantum» peak (2Q) as a function of the angle φ_h. Points are experimental data, the solid line is function $\cos^2 \varphi_h$, the dashed line is constant

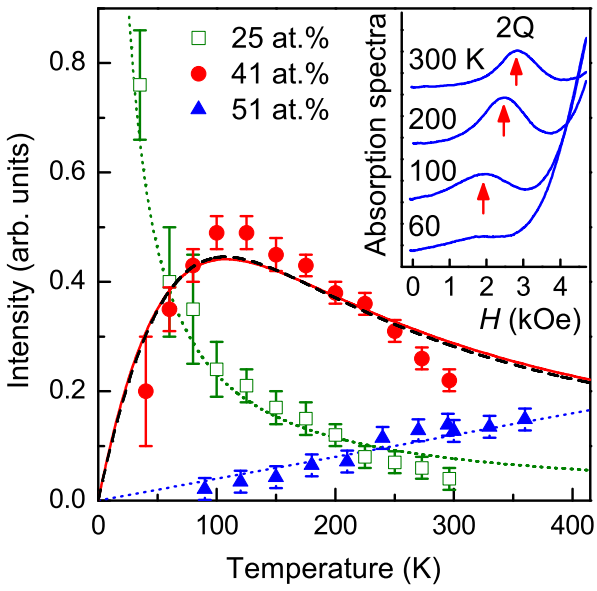

Fig. 2. Temperature dependencies of integral intensity for the «double quantum» peak in nanocomposite films $(CoFeB)_x(Al_2O_3)_{100-x}$ ($x \approx 25$–51 at. %). Symbols are experimental data obtained at frequency $f \approx 25$ GHz. Dotted lines are the Curie law $\propto T^{-1}$ (for $x \approx 25$ at. %) and linear dependence (for $x \approx 51$ at. %). Solid and dashed lines correspond to Eqs. (11) and (13) respectively. The inset demonstrates the shape of the «double quantum» peak (2Q) at different temperatures for the film with $x \approx 41$ at. %

Figure 2 demonstrates different types of experimental dependencies $I_2(T)$ for nanogranular films CoFeB–Al_2O_3 with various content of the FM phase x, which confirm the theoretical predictions. At low x («small» magnetic particles $\mu \sim 10^2\mu_B$, where μ_B is Bohr magneton), we observe the Curie law $I_2(T) \propto T^{-1}$ down to $T \approx 10$ K. Near the percolation threshold («large» magnetic particles $\mu \sim 10^4\mu_B$), the dependence $I_2(T)$ is linear up to highest studied temperature (360 K). For intermediate concentrations, the dependencies $I_2(T)$ are non-monotonic in qualitative agreement with Eq. (11). The typical magnetic moment of particles $\mu \sim 10^3\mu_B$ corresponds to $T_{max} \sim 100$ K.

Note that here we performed detailed consideration of «double quantum» excitations in non-interacting anisotropic granules. Another possible reason for realization of such excitations is the presence of weak dipole-dipole interactions between particles. The properties of the «double quantum» peak in this case prove to be qualitatively similar. The expression for the double-frequency amplitudes A_{2i}, A_{2j} of interacting particles i, j has the same structure as Eq. (3) (see Appendix):

$$A_{2i,j} = \frac{1}{4}\frac{H_D}{H} A_{1i} A_{1j}\, p(\theta_{ij}), \tag{12}$$

where $H_D = 3\mu/r_{ij}^3$ is an effective dipolar field at the distance r_{ij} between the particles ($H_D \ll H$), and θ_{ij} is the angle between $\mathbf{r}_{ij}$ and $\mathbf{H}$. The coefficient «3» in the expression for H_D comes from anisotropic part of the dipolar energy. If the particles are located at random angles θ_{ij}, the intensity of the «double quantum» peak is proportional to

$$I_2^{dip} = \frac{1}{15}\left(\frac{H_D}{H}\right)^2 \frac{L^2(\varkappa)}{\varkappa} \tag{13}$$

(see also [6, 7]). The principal features of the function (13) coinside with those of Eq. (11). The similar temperature dependence has a maximum at about $T_{max} \approx 0.37\,\mu H/k_B$. In practice, the shapes of the curves (11) and (13) are very close to each other (Fig. 2).

It is important to note that at $T = 0$, the linear susceptibility χ'' vanishes at multiple resonance frequencies (in particular $I_2 = 0$, see Eqs. (11), (13)). Indeed, the case $T = 0$ corresponds to pure classical FM state of the particles. It is well-known that in this situation, the multiple-frequency resonances can be excited only in essentially non-linear regime [36, 37]. On the contrary, the presence of thermal magnetic fluctuations in particles at $T > 0$ initiates the non-zero linear response of the system at multiple resonance frequencies. We have checked experimentally that in our case, we deal with such linear dependence of absorption peak intensities on the applied MW power.

4. EFFECTS OF SAMPLE SHAPE

In previous section, the theoretical consideration of magnetic resonance in FM particles did not take into account the existence of long-range dipolar interactions in macroscopic ensembles of such particles. Meanwhile, these interactions are known to have significant effect on the resonance frequency when the average magnetization of the magnetic medium is sufficiently large comparing with the resonance field. In this case, the presence of long-range dipolar interactions («demagnetizing fields») results in additional shift of the resonance frequency depending on the shape of the sample.

Application of MW field at the main resonance frequency of the sample initiates a weak precession of its average magnetization $\mathbf{M}$. As a first «mean field» ap-

proximation, the precession frequency is determined by Landau – Lifshitz equation

$$d\mathbf{M}/dt = \gamma[\mathbf{H}_{eff}(\mathbf{M}), \mathbf{M}], \tag{14}$$

where the effective field $\mathbf{H}_{eff}(\mathbf{M})$ is a function of $\mathbf{M}$ depending on the sample shape. For random homogeneous distribution of magnetic particles, $\mathbf{H}_{eff}(\mathbf{M})$ is defined by demagnetizing tensor $\hat{\mathbf{N}}$ of the sample and the local Lorentz field $4\pi\mathbf{M}/3$ inside the granular medium [38]:

$$\mathbf{H}_{eff}(\mathbf{M}) = \mathbf{H} - \hat{\mathbf{N}}\mathbf{M} + 4\pi\mathbf{M}/3.$$

Note that this simplified «mean field» approach completely neglects the random distribution of local anisotropy and dipolar fields inside the medium. However, such simplification seems reasonable, taking into account relatively narrow and symmetric experimental resonance peaks (Fig. 1) indicating low influence of inhomogeneities. In the case of thin film, which is of particular interest for us, the expression for the effective field takes the form

$$\mathbf{H}_{eff}(\mathbf{M}) = \mathbf{H} - 4\pi\mathbf{M}_{\perp} + 4\pi\mathbf{M}/3, \tag{15}$$

where $\mathbf{M}_{\perp}$ is vector component of magnetization normal to the film plane. Finding eigenfrequencies of linearized Eq. (14), we come to usual Kittel formulae for FMR frequencies at different orientations of the field $\mathbf{H}$ with respect to the film plane:

$$\begin{aligned} \omega_{\parallel}^{FMR} &= \gamma\sqrt{H(H+4\pi M)} \quad \text{for } \mathbf{H} \parallel \text{plane}, \\ \omega_{\perp}^{FMR} &= \gamma(H - 4\pi M) \quad \text{for } \mathbf{H} \perp \text{plane}. \end{aligned} \tag{16}$$

Experimental absorption spectra of nanogranular films clearly demonstrate the effects of demagnetizing fields on the resonance peak positions (Fig. 3). In the limit of low FM phase contents, the resonance fields for both absorption peaks are independent on the magnetic field orientation θ_H with respect to the film plane. The position of the main «FMR» peak formally corresponds to the effective g-factor $g_{eff} \approx 2.1$ which is typical of CoFeB alloy. The position of the «double quantum» peak corresponds to double effective g-factor $g_{eff} \approx 4.2$.

As the FM phase content grows, both peaks demonstrate pronounce angular dependence of the resonance field. For the main peak, the angular dependencies are well described by usual equation system for FMR [39]

$$\begin{aligned} \omega^2/\gamma^2 &= [H\cos(\theta_H - \theta_M) - 4\pi M \sin^2\theta_M] \times \\ &\times [H\cos(\theta_H - \theta_M) + 4\pi M \cos 2\theta_M], \\ 2H\sin(\theta_H - \theta_M) &= 4\pi M \sin 2\theta_M, \end{aligned} \tag{17}$$

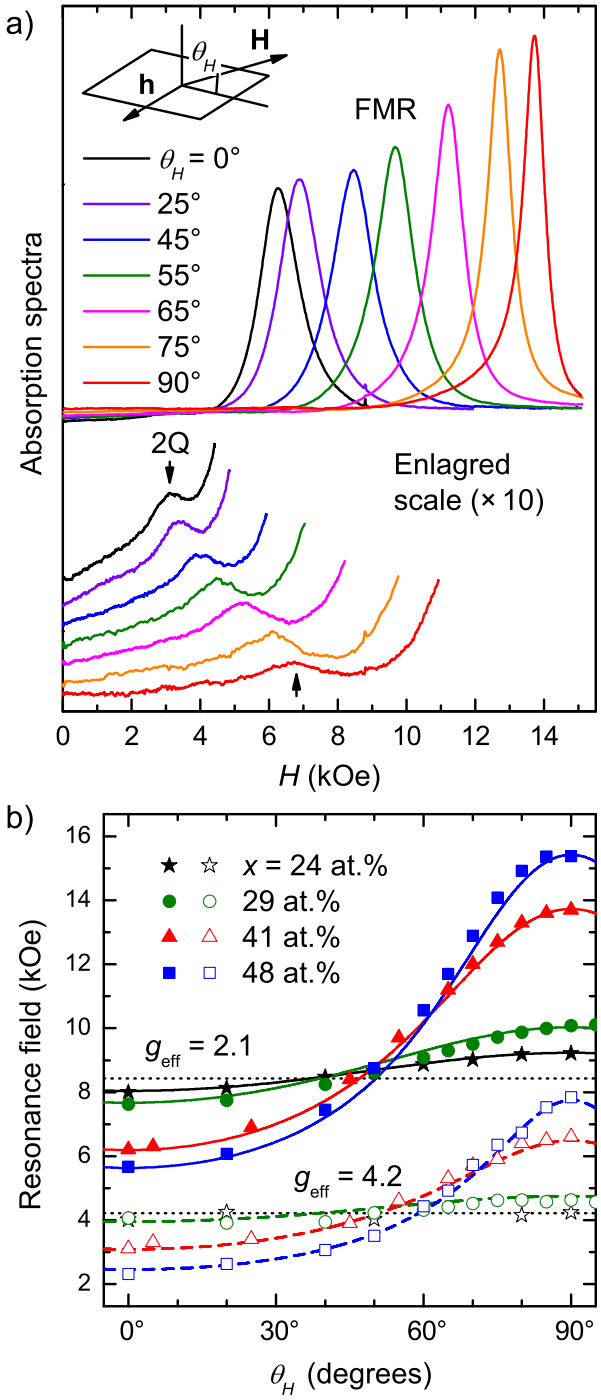

Fig. 3. *a* — Room temperature absorption spectra for the film $(CoFeB)_{41}(Al_2O_3)_{59}$ at a frequency $f \approx 25.0$ GHz and different orientations θ_H of the external field with respect to the film plane. *b* — Resonance field as a function of the angle θ_H for the FMR line ($g_{eff} \approx 2.1$, solid symbols) and the «double quantum» peak ($g_{eff} \approx 4.2$, open symbols) in nanogranular films CoFeB–Al_2O_3 with different FM phase content x. Symbols are experimental data, lines are their approximation (see text)

where the second equation defines the equilibrium orientation θ_M of the magnetization vector $\mathbf{M}$ with respect to the film plane.

For the «double quantum» peak, the situation proves to be more interesting. The naive approach would suggest that the resonance frequency for this peak should be just double the FMR frequency. Indeed, it would be the case if we considered excitation of FMR in a single FM particle. However, this naive idea is not confirmed experimentally for the investigated nanogranular films. This fact is better to illustrate considering frequency-field dependencies $f(H)$ obtained in two experimental geometries for samples with high $4\pi M$ values.

Figure 4 demonstrates dependencies $f(H)$ for CoFeB–Al_2O_3 nanogranular film with high concentration of the FM phase $x \approx 48$ at. %. The behavior of the main (FMR) peak is well described by Kittel Eqs. (16). Note that in contrast to the case of pure ferromagnet with constant magnetization, we must take into account the field dependence $4\pi M(H)$ due to superparamagnetic effect. Within the «mean field» approach, the value $4\pi M$ in Eqs. (16) is defined by Langevin function of the effective field (15) depending on the field direction [40, 41]:

$$4\pi M = 4\pi M_S L\left(\frac{\mu H_{eff}}{k_B T}\right), \qquad (18)$$

where M_S is saturation magnetization and

$$H_{eff} = \begin{cases} H + 4\pi M/3 & \text{for } \mathbf{H} \parallel \text{plane}, \\ H - 8\pi M/3 & \text{for } \mathbf{H} \perp \text{plane}. \end{cases} \qquad (19)$$

Eqs. (18), (19) define the function $4\pi M(H)$ implicitly. In practice, it is convenient to consider H_{eff} as a parameter. Then the function $4\pi M(H)$ can be easily plotted in parametric form.

In Fig. 4*b*, the experimental dependencies $4\pi M(H)$ obtained from FMR data using Eqs. (16) are well approximated by Eqs. (18), (19) with parameters $4\pi M_S \approx 7.7$ kOe and $\mu \approx 4.1 \cdot 10^3\,\mu_B$. Solid lines in Fig. 4*a* are the resulting approximation of the frequency-field dependencies for the FMR line by Eqs. (16), (18), (19).

The dotted lines in Fig. 4*a* correspond to double FMR frequencies ($2\omega_{\parallel}^{FMR}$ and $2\omega_{\perp}^{FMR}$). In parallel geometry, they describe the experimental frequency-field dependence of the «double quantum» peak satisfactorily. However, there is a clear discrepancy with the experiment in the normal geometry. The reason for this is following.

Note that under FMR conditions, a coherent precession of the average magnetization $\mathbf{M}$ is excited in the film. In this case, in the Landau – Lifshitz equations describing this precession, the torque associated with the Lorentz field vanishes: $[4\pi\mathbf{M}/3, \mathbf{M}] = 0$. Thus, the Lorentz field is absent in the Kittel formulae describing the behavior of the usual FMR line in thin films.

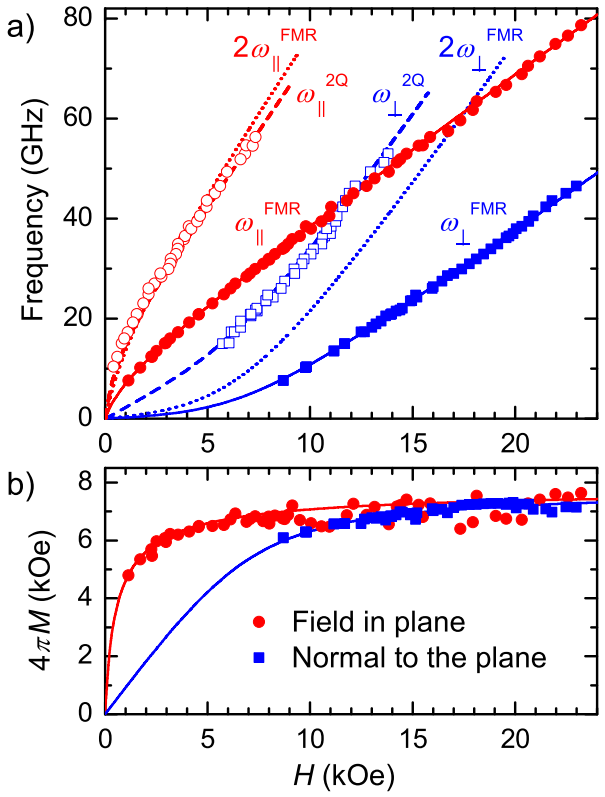

Fig. 4. *a* — Frequency-field dependencies $f(H)$ for the FMR line (ω^{FMR}) and the «double quantum» peak (ω^{2Q}) in the $(CoFeB)_{48}(Al_2O_3)_{52}$ film when the magnetic field is applied in the sample plane (red circles) and normal to the plane (blue squares). *b* — Field dependencies of demagnetizing field $4\pi M$. Symbols are experimental data (room temperature), lines are calculations (see text)

On the contrary, when exciting the resonance at the double frequency, the precession phases of individual particles at the main frequency have a random character (the phase shifts between the first and second harmonics are defined by random orientations of anisotropy axes in the particles). Under these conditions, the coherent precession of the average magnetization $\mathbf{M}$ is absent, and the frequency ω_{2Q} is simply determined by the static value of the effective field H_{eff}:

$$\omega_{2Q} = 2\gamma H_{eff}. \qquad (20)$$

In particular, for simple experimental geometries «field in plane» and «field normal to the plane», we get

$$\omega_{\parallel}^{2Q} = 2\gamma\,(H + 4\pi M/3) \quad \text{for } \mathbf{H} \parallel \text{plane},$$
$$\omega_{\perp}^{2Q} = 2\gamma\,(H - 8\pi M/3) \quad \text{for } \mathbf{H} \perp \text{plane}. \qquad (21)$$

Dashed lines in Fig. 4 *a* are plotted in accordance with Eqs. (21) taking into account the dependencies $4\pi M(H)$ obtained from FMR data. As it is seen, these formulae perfectly describe the experimental data for the «double quantum» peak without additional fitting parameters. Thus, in contrast to FMR, the resonance at the double harmonic reveals the presence of the Lorentz field in the film.

Eqs. (15), (20) also allow to calculate the resonance field of the «double quantum» peak for arbitrary field orientation with respect to the film plane:

$$H_r(\theta_H) = \left[\frac{\cos^2\theta_H}{(H_0 - H_L)^2} + \frac{\sin^2\theta_H}{(H_0 + 2H_L)^2}\right]^{-1/2}, \qquad (22)$$

where $H_0 = \omega/2\gamma$ and $H_L = 4\pi M/3$. In Fig. 3 *b*, the experimental dependencies $H_r(\theta_H)$ for this peak are well fitted by Eq. (22), while the FMR data are approximated by Eqs. (17).

Similarly, both frequency-field and orientational dependencies for the film $(CoFeB)_{60}(SiO_2)_{40}$ are well described within the proposed approach (Fig. 5). It is interesting, that the content of the FM phase is above the percolation threshold for this sample, and its magnetization is almost field independent $4\pi M \approx 4\pi M_S$. However this sample still demonstrates the presence of the «double quantum» peak, which seems due to existence of isolated FM nanogranules in the film besides the macroscopic percolation clusters.

As a result, the entire set of experimental curves in Fig. 5 is perfectly fitted using only two parameters: $4\pi M \approx 8.6$ kOe and the gyromagnetic ratio $\gamma/2\pi \approx 2.96$ GHz/kOe ($g_{eff} \approx 2.1$). The FMR data are approximated by the conventional Kittel equations (16, 17), while the behavior of the «double quantum» peak is described by Eqs. (21), (22) taking into account the Lorentz field in the film. For comparison, the dotted line in Fig. 5 *b* is plotted according to Eqs. (17) for FMR with double *g*-factor $g_{eff} \approx 4.2$. Clearly, Eq. (22) works much better (the dashed line).

In the end, we would like to discuss one more interesting experimental result concerning the «double quantum» peak. As it is seen in Figs. 4, 5, this peak disappears in the region of high frequencies $f > 60$ GHz. This effect becomes clear if we consider Eqs. (11), (13) for the intensity of the «double quantum» excitations I_2. Indeed, according to these expressions, I_2 should decrease rapidly with increasing field. In the limit of high fields, the ratio I_2/I_1 should follow the law $I_2/I_1 \propto H^{-3}$. Now we must remember that within our «mean field» approach, the magnetic field H must be replaced by the effective field H_{eff} inside the film. But according to Eq. (20), H_{eff} is proportional to the measuring frequency f. Thus, the ratio of integral intensi-

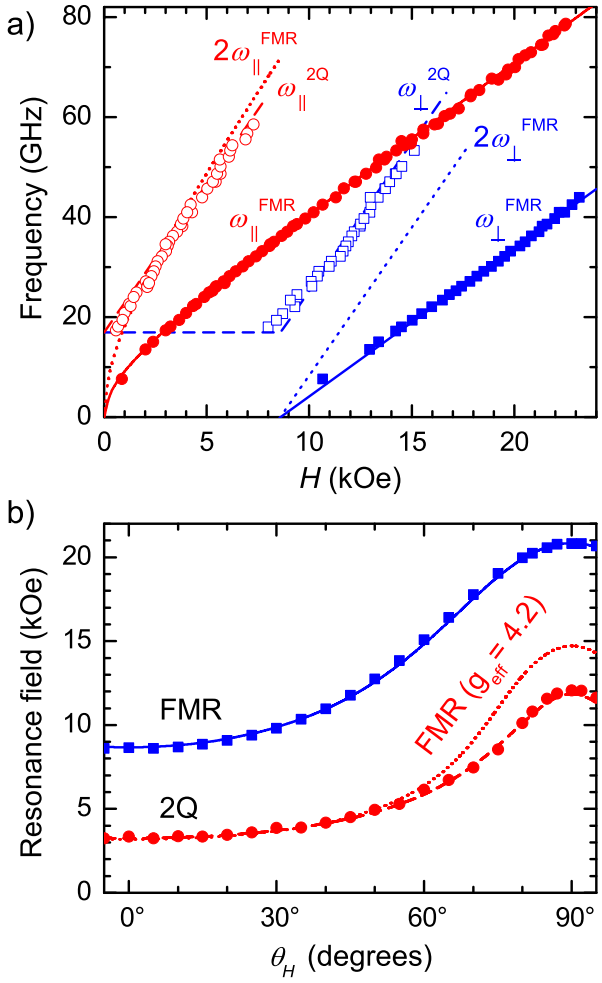

Fig. 5. *a* — Frequency-field dependencies $f(H)$ for the FMR line (ω^{FMR}) and the «double quantum» peak (ω^{2Q}) in the $(CoFeB)_{60}(SiO_2)_{40}$ film when the magnetic field is applied in the sample plane (red circles) and normal to the plane (blue squares). *b* — Dependencies of the resonance fields for two peaks on the orientation of the magnetic field with respect to the film plane. Symbols are experimental data (room temperature, $f \approx 36.2$ GHz), lines are calculations (see text)

ties of the «double quantum» peak (I_{2Q}) and the FMR line (I_{FMR}) should follow the law $I_{2Q}/I_{FMR} \propto f^{-3}$.

Figure 6 demonstrates that this relation is indeed fulfilled at high frequencies. Note that the experimental points measured at different field orientations with respect to the film plane coincide within experimental accuracy. This result confirms the applicability of the used «mean field» approach: despite the essential difference in the resonance fields in two geometries, the intensity of the «double quantum» peak is defined only by the effective field inside the film H_{eff} which depends only on the experimental frequency f.

5. CONCLUSION

Using the method of electron spin resonance, we studied films of metal-insulator nanogranular composites CoFeB–Al_2O_3 and CoFeB–SiO_2 representing ensembles of metallic superparamagnetic particles CoFeB randomly distributed in insulating oxide matrices. The experimental spectra, besides the conventional FMR signal, contain an additional absorption peak demonstrating a number of unusual properties: double effective g-factor $g_{eff} \approx 4$, independence of the peak intensity on the resonance excitation geometry (transverse or longitudinal), and non-monotonic dependencies of its intensity on temperature.

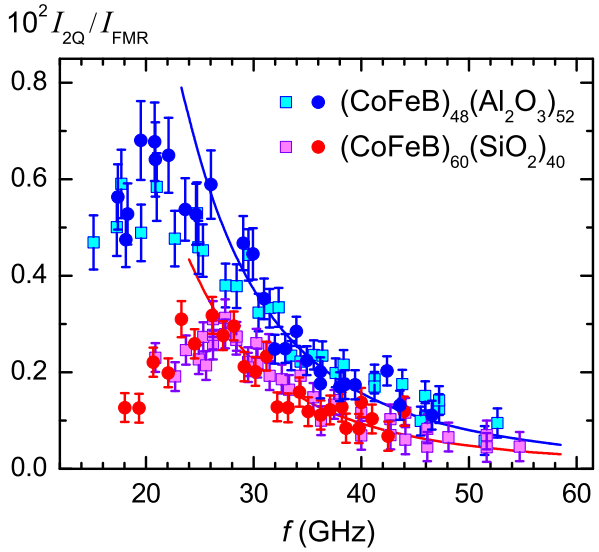

Fig. 6. Ratio of integral intensities of the «double quantum» peak and the FMR line (I_{2Q}/I_{FMR}) as a function of resonance excitation frequency f. Experimental data are shown for two films of different compositions for the magnetic field applied parallel (squares) and normal (circles) to the film plane. Lines are dependencies $I_{2Q}/I_{FMR} \propto f^{-3}$

The observed peculiar features of the experimental spectra are similar to those found for iron oxide particles in polymer media in a set of works [5–12]. In these works, the magnetic resonance spectra were treated in terms of quantum mechanical «giant spin» model, considering FM particles as PM centers with very large spins $S \sim 10^2$–10^4. The appearance of «anomalous» peak with a double effective g-factor was explained by the excitation of double quantum transitions in these PM centers with a change in the spin projection $\Delta m = \pm 2$.

In contrast to these previous works, here we proposed pure classical approach to treat the «multiple quantum» excitations in magnetic particles. Within this approach, the absorption of MW power by classical magnetic moments occurs at multiple harmonics of their precessional motion. This effect is possible when the circular precession of the magnetic moment is disturbed in the presence of magnetic anisotropy or dipole-dipole interactions between the particles. It is important that ensembles of superparamagnetic particles demonstrate a linear response to the MW field at multiple resonance frequencies, in contrast to a macroscopic ferromagnet. Both the quantum mechanical «giant spin» and the classical approaches are equivalent. The choice of one or another model can be made for reasons of convenience.

The observed experimental features of the magnetic resonance spectra are well explained within the proposed theoretical concepts. In particular, we note the principally different influence of long-range dipolar fields on the resonance frequencies for the conventional FMR line and the «double quantum» peak. Besides the usual demagnetizing fields, the presence of the Lorentz field in nanogranular films leads to an observed additional frequency shift of the «double quantum» peak.

Acknowledgements. The authors thank V. I. Marchenko, F. S. Dzheparov, and V. A. Atsarkin for helpful comments and stimulating discussions.

Funding. The work was carried out within the framework of a State Assignment and was financially supported by the Russian Science Foundation (project № 22-12-00259-П).

Conflict of interest. The authors of this work declare that they have no conflicts of interest.

Author's contributions. The contribution of the authors is equivalent.

SOLUTION OF LANDAU – LIFSHITZ EQUATIONS

Magnetic particle with uniaxial anisotropy

We note, that the system of Landau – Lifshitz equations (5) can be reduced to a single differential equation of the second order. For this purpose, we need to consider new coordinate system rotated around y-axis by an angle θ so that the new axis z' is aligned with the anisotropy direction. In this new coordinate system, the energy of the particle (4) normalized to μH takes the form

$$\varepsilon = -m_z - a m_A^2 = -m_A \cos\theta + m_\perp \sin\theta - a m_A^2, \quad (23)$$

where $\varepsilon = E/\mu H$, $a = H_A/2H$, m_A and $m_\perp$ are the projections of unit magnetization vector onto axes z' and x' (parallel and perpendicular to the anisotropy axis). The Landau – Lifshitz equation for the component m_A takes the form

$$\dot{m}_A = -m_y \sin\theta. \quad (24)$$

The component m_y is determined from the condition $|\mathbf{m}| = 1$:

$$m_y = \pm\sqrt{1 - m_A^2 - m_\perp^2}. \quad (25)$$

The component $m_\perp$ can be expressed as a function of m_A from Eq. (23), using the condition of energy conservation $\varepsilon = \text{const}$:

$$m_\perp = (\varepsilon + m_A \cos\theta + a m_A^2)/\sin\theta. \quad (26)$$

Substituting (26) into (25) and then (25) into (24), we obtain the differential equation for m_A:

$$\dot{m}_A = \pm\sqrt{(1 - m_A^2)\sin^2\theta - (\varepsilon + m_A\cos\theta + a m_A^2)^2}.$$

Taking the second time derivative, the square root in the right part disappears, and we obtain a typical equation for one-dimensional anharmonic oscillator [32]:

$$\ddot{m}_A + b_0 + b_1 m_A + b_2 m_A^2 + b_3 m_A^3 = 0, \quad (27)$$

where $b_0 = \varepsilon\cos\theta$, $b_1 = 1 + 2\varepsilon a$, $b_2 = 3a\cos\theta$, $b_3 = 2a^2$. In the limit of small $a \ll 1$, its solution has the form of Fourier cosine series [32]

$$m_A = C_0 + C_1\cos\psi + C_2\cos 2\psi + \ldots \quad (28)$$

where $\psi = \omega t + \varphi$. The frequency ω and coefficients C_q can be defined by direct substitution of Eq. (28) into Eq. (27). In particular, in the first order in a, the second harmonic C_2 is connected with the main harmonic C_1 by expression

$$C_2 = \frac{b_2}{6}C_1^2 = \frac{a}{2}C_1^2\cos\theta.$$

The higher harmonics have higher order in a. The magnetization components m_α ($\alpha = x, y, z$) in the original coordinate system can be calculated from m_A using Eqs. (23), (24) and the relation

$$m_A = m_z\cos\theta + m_x\sin\theta.$$

They take the form of Fourier series (6) with second harmonic amplitudes given by

$$A_{2x,y} = a\,C_1^2\,\frac{\cos\theta}{\sin\theta}, \quad A_{2z} = -\frac{a}{2}C_1^2.$$

In zero approximation, the coefficient C_1 is connected with the main precession amplitude A_1 by expression $C_1 = A_1\sin\theta$. Thus, we reproduce Eqs. (9) for the second harmonic amplitudes which can also be obtained by direct substitution of Eqs. (6) into Landau – Lifshitz Eqs. (5) as it is shown in Section 3.2. In this way, of course, we can also reproduce Eqs. (7), (8) obtained in Section 3.2.

Two dipolar coupled magnetic particles

Let us consider Landau – Lifshitz equations without dissipation for two identical particles with magnetic moments $\boldsymbol{\mu}_i$ ($i = 1, 2$):

$$\frac{d\boldsymbol{\mu}_i}{dt} = \gamma\left[\mathbf{H}_i \times \boldsymbol{\mu}_i\right].$$

Here $\mathbf{H}_i$ is an effective field acting on the particle i, including dipolar field produced by the particle $j \neq i$:

$$\mathbf{H}_i = \mathbf{H} - \frac{\boldsymbol{\mu}_j}{r_{ij}^3} + \frac{3(\boldsymbol{\mu}_j\cdot\mathbf{r}_{ij})\mathbf{r}_{ij}}{r_{ij}^5},$$

where $\mathbf{r}_{ij}$ is a space vector from the particle i to j. Now we introduce a coordinate system such that z-axis is aligned in the direction of the external field $\mathbf{H}$, and the vector $\mathbf{r}_{ij}$ is oriented in the xz-plane at an angle θ_{ij} with z-axis. Introducing unit magnetization vectors $\mathbf{m}_i = \boldsymbol{\mu}_i/\mu$, dimensionless time $t' = \omega_0 t$ and a small parameter $c = \mu/Hr_{ij}^3$, the Landau – Lifshitz equations for the components m_{ix} and m_{iy} take form

$$\begin{aligned}
\dot{m}_{ix} &= -m_{iy} - c\,[p_1 m_{jz} m_{iy} + m_{iz} m_{jy} + p_3 m_{jx} m_{iy}],\\
\dot{m}_{iy} &= m_{ix} + c\,[p_1 m_{jz} m_{ix} - p_2 m_{iz} m_{jx} + \\
&\qquad + p_3 m_{jx} m_{ix} - p_3 m_{iz} m_{jz}],
\end{aligned} \quad (29)$$

where

$$p_1 = 3\cos^2\theta_{ij} - 1, \quad p_2 = 3\sin^2\theta_{ij} - 1,$$

$$p_3 = 3\sin\theta_{ij}\cos\theta_{ij}.$$

In «zero» approximation ($c = 0$), the solution of Eqs. (29) represents two independent harmonic oscillators:

$$m_{ix}^{(0)} = A_{1i}\cos\psi_i, \quad m_{iy}^{(0)} = A_{1i}\sin\psi_i,$$

where $\psi_i = \omega_i t + \varphi_i$. In the presence of weak interaction, we obtain two coupled nonlinear oscillators. The general solution can be non-periodic with amplitudes and phases being «slow» time-dependent functions. At small time scales, as a first approximation, the relation between first and second harmonics can be found by substitution:

$$\begin{aligned} m_{ix} &= A_{1i}\cos\psi_i + A_{2ix}\cos(\psi_1+\psi_2) + c\,(...), \\ m_{iy} &= A_{1i}\sin\psi_i + A_{2iy}\sin(\psi_1+\psi_2) + c\,(...). \end{aligned} \tag{30}$$

Here the second harmonic amplitudes $A_2 \sim c$, and $c\,(...)$ stands for other weak combination harmonics which are of no interest for us. The components m_{iz} appear in Eqs. (29) in combinations $\sim c m_{iz}$. Thus, in the first order in c, we can put $m_{iz} = \bar{m}_{iz} = \text{const}$. After substitution of Eqs. (30) into Eqs. (29), we get

$$A_{2ix,y} = \frac{1}{2} c p_3 A_{1i} A_{1j} = \frac{1}{4}\frac{H_D}{H} A_{1i} A_{1j} \sin 2\theta_{ij}, \tag{31}$$

where $H_D = 3\mu/r_{ij}^3$. The component m_{iz} can be calculated integrating the third Landau – Lifshitz equation

$$\dot{m}_{iz} = c\left[p_3 m_{jz} m_{iy} + p_2 m_{jx} m_{iy} + m_{ix} m_{jy}\right].$$

Substituting Eqs. (30) to the right part, we obtain for the second harmonic:

$$\begin{aligned} A_{2iz} &= -\frac{1}{4} c\,(p_2+1)\, A_{1i} A_{1j} = \\ &= -\frac{1}{4}\frac{H_D}{H} A_{1i} A_{1j} \sin^2\theta_{ij}. \end{aligned} \tag{32}$$

Thus, Eqs. (31), (32) lead to Eq. (12).

REFERENCES

1. *Magnetic Properties of Fine Particles*, ed. by J. L. Dormann and D. Fiorani, Elsevier, Amsterdam (1992).
2. *Magnetic Nanoparticles*, ed. by S. P. Gubin, Wiley, Hoboken, NJ (2009).
3. S. Bedanta, A. Barman, W. Kleemann, O. Petracic, and T. Seki, J. Nanomater. **2013**, 952540 (2013).
4. N. Noginova, F. Chen, T. Weaver, E. P. Giannelis, A. B. Bourlinos, and V. A. Atsarkin, J. Phys. Condens. Matter **19**, 246208 (2007).
5. M. M. Noginov, N. Noginova, O. Amponsah, R. Bah, R. Rakhimov, and V. A. Atsarkin, J. Magn. Magn. Mater. **320**, 2228 (2008).
6. N. Noginova, T. Weaver, E. P. Giannelis, A. B. Bourlinos, V. A. Atsarkin, and V. V. Demidov, Phys. Rev. B **77**, 014403 (2008).
7. N. Noginova, Yu. Barnakov, A. Radocea, and V. A. Atsarkin, J. Magn. Magn. Mater. **323**, 2264 (2011).
8. N. Noginova, B. Bates, and V. A. Atsarkin, Appl. Magn. Reson. **47**, 937 (2016).
9. M. Fittipaldi, R. Mercatelli, S. Sottini, P. Ceci, E. Falvo, and D. Gatteschi, Phys. Chem. Chem. Phys. **18**, 3591 (2016).
10. A. Cini, P. Ceci, E. Falvo, D. Gatteschi, and M. Fittipaldi, Z. Phys. Chem. **231**, 745 (2017).
11. N. E. Domracheva, V. E. Vorobeva, M. S. Gruzdev, Y. N. Shvachko, and D. V. Starichenko, Inorg. Chim. Acta **465**, 38 (2017).
12. V. A. Atsarkin and N. Noginova, Appl. Magn. Reson. **51**, 1467 (2020).
13. A. B. Drovosekov, N. M. Kreines, O. A. Kovalev, A. V. Sitnikov, S. N. Nikolaev, and V. V. Rylkov, J. Exp. Theor. Phys. **134**, 725 (2022).
14. A. B. Drovosekov, N. M. Kreines, O. A. Kovalev, A. V. Sitnikov, S. N. Nikolaev, and V. V. Rylkov, J. Exp. Theor. Phys. **135**, 372 (2022).
15. A. B. Drovosekov, N. M. Kreines, D. A. Ziganurov, A. V. Sitnikov, S. N. Nikolaev, and V. V. Rylkov, J. Exp. Theor. Phys. **137**, 562 (2023).
16. A. B. Drovosekov, M. Yu. Dmitrieva, A. V. Sitnikov, S. N. Nikolaev, and V. V. Rylkov, J. Exp. Theor. Phys. **166**, 383 (2024) [arXiv:2406.04799].
17. Yu. A. Koksharov, D. A. Pankratov, S. P. Gubin, I. D. Kosobudsky, M. Beltran, Y. Khodorkovsky, and A. M. Tishin, J. Appl. Phys. **89**, 2293 (2001).
18. I. Edelman, O. Ivanova, R. Ivantsov, D. Velikanov, V. Zabluda, Y. Zubavichus, A. Veligzhanin, V. Zaikovskiy, S. Stepanov, A. Artemenko, J. Curély, and J. Kliava, J. Appl. Phys. **112**, 084331 (2012).
19. T. Castner, G. S. Newell, W. C. Holton, and C. P. Slichter, J. Chem. Phys. **32**, 668 (1960).
20. H. H. Wickman, M. P. Klein, and D. A. Shirley, J. Chem. Phys. **42**, 2113 (1965).
21. A. Granovsky, Yu. Kalinin, A. Sitnikov, and O. Stognei, Phys. Procedia **82**, 46 (2016).

22. V. V. Rylkov, S. N. Nikolaev, K. Yu. Chernoglazov, V. A. Demin, A. V. Sitnikov, M. Yu. Presnyakov, A. L. Vasiliev, N. S. Perov, A. S. Vedeneev, Yu. E. Kalinin, V. V. Tugushev, and A. B. Granovsky, Phys. Rev. B **95**, 144202 (2017).

23. O. V. Stognei and A. V. Sitnikov, Phys. Solid State **52**, 2518 (2010).

24. V. V. Rylkov, A. V. Emelyanov, S. N. Nikolaev, K. E. Nikiruy, A. V. Sitnikov, E. A. Fadeev, V. A. Demin, and A. B. Granovsky, J. Exp. Theor. Phys. **131**, 160 (2020).

25. O. V. Stognei, Yu. E. Kalinin, A. V. Sitnikov, I. V. Zolotukhin, and A. V. Slyusarev, Phys. Met. Metallogr. **91**, 21 (2001).

26. A. Abragam and B. Bleaney, *Electron Paramagnetic Resonance of Transition Ions*, Clarendon Press, Oxford (1970).

27. S. A. Altshuler and B. M. Kozyrev, *Electron Paramagnetic Resonance in Compounds of Transition Elements*, Wiley, New York (1974).

28. C. Marti, R. Romestain, and R. Visocekas, Phys. Status Solidi **28**, 97 (1968).

29. B. Clerjaud, Phys. Status Solidi B **72**, K33 (1975).

30. L. D. Landau and E. M. Lifshitz, *Course of Theoretical Physics, Vol. 3, Quantum Mechanics: Non-Relativistic Theory*, Pergamon Press, Oxford (1977).

31. N. N. Bogoliubov and Yu. A. Mitropolsky *Asymptotic Methods in the Theory of Nonlinear Oscillations*, Gordon and Breach, New York (1961).

32. L. D. Landau and E. M. Lifshitz, *Course of Theoretical Physics, Vol. 1, Mechanics*, Butterworth-Heinemann, Oxford (1976).

33. L. D. Landau and E. M. Lifshitz, *Course of Theoretical Physics, Vol. 5, Statistical Physics*, Pergamon Press, Oxford (1980).

34. R. M. White, *Quantum Theory of Magnetism*, Springer, Berlin (2007).

35. J. S. Smart, *Effective Field Theories in Magnetism*, Saunders, London (1966).

36. D. D. Douthett, I. Kaufman, and A. S. Risley, J. Appl. Phys. **32**, 1905 (1961).

37. A. B. Petrovskii, Theor. Math. Phys. **2**, 184 (1970).

38. J. Dubowik, Phys. Rev. B **54**, 1088 (1996).

39. R. Soohoo, *Magnetic Thin Films*, Harper and Row, New York (1965).

40. M. Godinho, J. L. Dormann, M. Noguès, P. Prené, E. Tronc, and J. P. Jolivet, J. Magn. Magn. Mater. **140–144**, 369 (1995).

41. J. L. Dormann and D. Fiorani, J. Magn. Magn. Mater. **140–144**, 415 (1995).